Iranian Journal of Chemical Engineering
Vol. 2, No. 2, 2005, IAChE

The effect of wall strengtheners on the performance of double-stage electrostatic precipitators

M. R. Talaie
Isfehan University, Chemical Engineering Department, Isfehan, Iran.

Abstract
The presence of wall strengtheners in double-stage electrostatic precipitators affects gas velocity, electrical field and particle movement over the ESP. In this work we have used our previous mathematical model for double-stage ESP {Talaie et. al (2001) [10]} to study the effect of wall strengtheners on the performance of double-stage ESP. One of the important findings was that, due to the fact that wall strengtheners increase the degree of turbulence, the effect of gas turbulence on particle movement can not be ignored. The results of the calculations show that the simple Lagrangian model in which this effect is neglected is not suitable, whereas using an Eulerian approach provides much better results. The results of this model also revealed that the collection efficiency for small particles increases while that for large particles decreases when a baffle is used as wall strengthener.

Keywords: *Mathematical model, Electrostatic precipitators, Wall strengtheners, Electrical field*

Introduction
Pollution, especially air pollution is one of the most important problems constraining the development of industries for many years. Suspended solid particles in flue gases may seriously endanger human health. In this connection, many attempts have been made to develop new technologies and more effective equipment to remove small particles from a gas stream. Among the equipment for particle removal, electrostatic precipitators are the most effective. Electrostatic precipitators (ESP) are widely used to remove fine particulates from gas streams in many industries such as cement production units and power stations. One essential difference between ESP and other kinds of equipment lies on the nature of the forces acting on particles. In ESP the removal force is due to attraction of charged particles in an electric field toward collecting plates. Particles moving along the fluid are dispersed due to velocity fluctuations while they are driven to collecting plates by Coulomb force.

One of the most important parameters influencing the electrostatic precipitation process is the gas flow pattern before and along ESP channels. Serious non-uniformity in gas flow pattern may tend to lower the ESP efficiency. The strengtheners of the collecting wall can affect both gas flow and electrical fields through the ESP. Due to mechanical strength strengtheners are usually used on collecting walls. The wall strengtheners can act as baffles against the gas flow and hence distort the flow pattern and electrical field. Figure 1 shows the simple configuration of a collecting wall. The effect of such baffles on ESP performance has been explained in several investigations, but the results are somewhat different. Lowe (1969) [5] has reported that the ESP performance for a flat collecting wall is less than that for a structured collecting wall. He has demonstrated that this effect may be attributed to the recirculation and turbulence produced by the baffles. Vincent and MacLennan (1980) [12] concluded that introducing baffles may improve ESP performance. Leonard et. al (1982)[4] performed an experimental examination of double-stage ESP performance and showed that baffles reduce ESP performance significantly due to introducing turbulence in gas flow. Stenhouse and Barnes (1990)[7] have described the positive effect of obstructions on ESP performance. Suh and Kim (1995[8], 1996[9]) have studied the effect of baffles on ESP performance by performing a numerical calculation. They have also used a Lagrangian method without considering the effect of fluctuations on particle dispersion to study the effect of obstructions on double-stage ESP performance. Also, they have ignored the effect of particle charge density on electrical field and fluid flow. They have interpreted this effect by means of two dimensionless numbers (Stokes and electrostatic numbers). They have concluded that the baffles may have a positive effect on ESP performance depending on the values of these numbers.

In the present work, a modified Eulerian model was developed to investigate the effect of wall strengtheners on double-stage ESP performance. This model is capable of considering the influence of gas velocity fluctuations on particle dispersion and the effect of particle charge density on fluid flow and electrical field. Also, by using a new approach the effect of particle size distribution could be included in the model. After validating the model by using the experimental data of Leonard et. al (1982) [4], it was used to evaluate the effect of depth and number of strengtheners on ESP performance for a wide range of relevant parameters.

Mathematical model

1) Eulerian approach

In this paper some important sections of the model are introduced. More details of development of this model is given by Talaie et. al (2001) [10].

The particle continuity equation was modified by introducing the number frequency distribution of particle size. As a result of this modification, the following equation for polydisperse particles was obtained:

$$\frac{\partial\left(u_P C_P(D_P)\right)}{\partial x}+\frac{\partial\left(v_P C_P(D_P)\right)}{\partial y}= \frac{\partial}{\partial x}\left(E_P\frac{\partial C_P(D_P)}{\partial x}\right)+\frac{\partial}{\partial x}\left(E_P\frac{\partial C_P(D_P)}{\partial x}\right)+S_G\,C_{P0}(D_P)-S_C C_{Pn}(D_P) \quad (1)$$

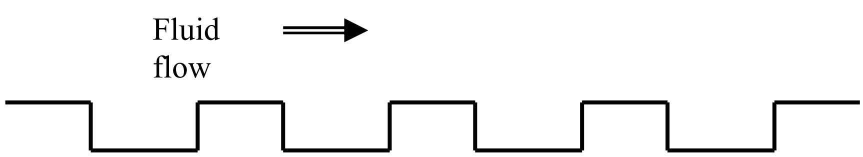

Figure 1. The simple structure of collecting electrode in an ESP

Where $C_P(D_P)$ is the number frequency distribution of particle size ($C_P(D_P)dD_P$ is the number concentration of particles having diameters between D_P and D_P+dD_P) and $C_{P0}(D_P)$ is the number frequency distribution of particle size at the entrance and may be considered as a log-normal distribution which can be obtained by the following relation:

$$C_{P0}(D_P) = \frac{C_{P0t}}{\sqrt{2\pi}D_P \ln(s)} EXP\left[\frac{-(\ln\frac{D_P}{\overline{D}_P})^2}{2(\ln s)^2}\right] \qquad (2)$$

It should be mentioned that other size distribution relations or even a numerical size distribution can be used for $C_{P0}(D_P)$ if necessary.
The following section will explain methods used to evaluate various parameters used in equation 1.

a- Eddy diffusivity, Ed:
The following equation proposed by Tennekes and Lumly (1972) [11] was used to predict the gas diffusion coefficient, Ep:

$$E_P = C u' l \qquad (3)$$

where C is a constant, u' is mean fluctuation velocity, l is the characteristic length usually defined in terms of ε, as follows {Leonard (1982) [4]}:

$$l = \frac{3u'^3}{2\varepsilon} \qquad (4)$$

u' can be set equal to $\sqrt{k}$, where k is the turbulent kinetic energy.

b- Particle velocity distribution
The following equations expressing momentum balance over particles can be used to evaluate the trajectory of particles:

$$\begin{cases} \frac{du_P}{dt} = \frac{3\rho_f}{4D_P\rho_P} C_{Df}\left|U - U_P\right|(u - u_P) + \frac{Q_P(D_P)}{m_P}E_x \\ \frac{dv_P}{dt} = \frac{3\rho_f}{4D_P\rho_P} C_{Df}\left|U - U_P\right|(v - v_P) + \frac{Q_P(D_P)}{m_P}E_y \end{cases} \qquad (5)$$

In this study it was assumed that particles acquire their terminal velocity instantaneouly. By using this assumption the particle velocity at each point can be equal to the terminal velocity coresponding to the fluid velocity. Therefore, in order to obtain the particle terminal velocity, the above momentum equations of particles were solved for u_P and v_P by taking $\frac{du_P}{dt} = 0$ and $\frac{dv_P}{dt} = 0$.
The correlation of Sartor and Abbott (1975) [6] for the drag coefficient, which was also used by Goo and Lee (1997) [2] to simulate ESP process, was applied in the present model:

$$\begin{cases} C_{Df} = \frac{24}{Re_P} & Re_P < 0.1 \\ C_{Df} = \frac{24}{Re_P}(1 + 0.0916\,Re_P) & 0.1 < Re_P < 5.0 \\ C_{Df} = \frac{24}{Re_P}(1 + 0.158\,Re_P^{2/3}) & 5.0 < Re_P < 1000 \end{cases} \qquad (6)$$

c - Gas velocity distribution
In order to predict fluid velocity distribution, the normal k-ε turbulent flow model was used. For two-dimensional incompressible steady flow and considering the electrical body force, the equations describing momentum and mass balance are as follows:

$$\frac{\partial}{\partial x}\left[\rho_f u^2-(\mu+\mu_t)\frac{\partial u}{\partial x}\right]+\frac{\partial}{\partial y}\left[\rho_f uv-(\mu+\mu_t)\frac{\partial u}{\partial y}\right]= -\frac{\partial p}{\partial x}+\frac{\partial}{\partial x}\left(\mu_t\frac{\partial u}{\partial x}\right)+\frac{\partial}{\partial y}\left(\mu_t\frac{\partial v}{\partial x}\right)+\int_{D_{P\min}}^{D_{P\max}} Q_P(D_P)E_x C_P(D_P)\,dD_P \quad (7)$$

$$\frac{\partial}{\partial x}\left[\rho_f uv-(\mu+\mu_t)\frac{\partial v}{\partial x}\right]+\frac{\partial}{\partial y}\left[\rho_f v^2-(\mu+\mu_t)\frac{\partial v}{\partial y}\right]= -\frac{\partial p}{\partial y}+\frac{\partial}{\partial x}\left(\mu_t\frac{\partial u}{\partial y}\right)+\frac{\partial}{\partial y}\left(\mu_t\frac{\partial v}{\partial y}\right)+\int_{D_{P\min}}^{D_{P\max}} Q_P(D_P)E_y C_P(D_P)\,dD_P \quad (8)$$

$$\frac{\partial(\rho_f u)}{\partial x}+\frac{\partial(\rho_f v)}{\partial y}=0 \quad (9)$$

$$\frac{\partial}{\partial x}(\rho_f uk)+\frac{\partial}{\partial y}(\rho_f uk)=\frac{\partial}{\partial x}\left(\frac{\mu_t}{\sigma_k}\frac{\partial k}{\partial x}\right)+\frac{\partial}{\partial y}\left(\frac{\mu_t}{\sigma_k}\frac{\partial k}{\partial y}\right)+\mu_t G-C_D\rho_f\varepsilon \quad (10)$$

$$\frac{\partial}{\partial x}(\rho_f u\varepsilon)+\frac{\partial}{\partial y}(\rho_f u\varepsilon)=\frac{\partial}{\partial x}\left(\frac{\mu_t}{\sigma_\varepsilon}\frac{\partial \varepsilon}{\partial x}\right)+\frac{\partial}{\partial y}\left(\frac{\mu_t}{\sigma_\varepsilon}\frac{\partial \varepsilon}{\partial y}\right)+\frac{\varepsilon}{k}(C_1\mu_t G-C_2\rho_f\varepsilon) \quad (11)$$

$$G=2\left(\frac{\partial u}{\partial x}\right)^2+2\left(\frac{\partial v}{\partial y}\right)^2+\left(\frac{\partial u}{\partial y}+\frac{\partial v}{\partial x}\right)^2 \quad (12)$$

$$\mu_t=C_\mu\frac{\rho_f k^2}{\varepsilon} \quad (13)$$

In the momentum equations, $Q_P(D_P)$ is the electric charge of particles having diameter between D_P and D_P+dD_P, which is constant during the precipitation process for a double-stage ESP. The integral terms in the momentum equations show the force exerted on the fluid by particle movement. This relation is based on the assumption that particles reach their settling velocities instantaneously. By using this assumption the force exerted on the fluid by particles can be considered as an electrical force exerted on the particles.

The parameters used in the normal k-ε model are as follows:

σ_k	σ_ε	C_μ	C_D	C_1	C_2
1.0	1.3	0.09	1.0	1.44	1.92

d- Electric field strength distribution

In solving equations 6, 10 and 11 one needs to have the electrical field strength. The governing equation for the electric field in ESP is the Poisson equation which, is normally expressed in terms of voltage:

$$\frac{\partial^2\phi}{\partial x^2}+\frac{\partial^2\phi}{\partial y^2}=-\frac{\int_{D_{P\min}}^{D_{P\max}} Q_P(D_P)C_P(D_P)\,dD_P}{\varepsilon_0} \quad (14)$$

The electric field was found from the following equation:

$$\begin{cases} E_x = -\dfrac{\partial \phi}{\partial x} \\ E_y = -\dfrac{\partial \phi}{\partial y} \end{cases} \qquad (15)$$

e - Particle charge

In single-stage ESPs the charging and collecting of particles take place simu-ltaneously, so in order to predict ESP's performance one needs the current-voltage characteristics. In double-stage ESPs, polluted gas is passed through a high-voltage wire-plate channel in order to charge particles before entering the collection section. When the particle concentration of polluted gas is low particles will be charged to saturation. In this study, in order to find $Q_P(D_P)$, it was assumed that the particles reached to their saturation charge during the charging process. Thus, the particle charge, $Q_P(D_P)$, was obtained from the following equation given by White (1963) [13] for the saturation charge of a particle with diameter D_P:

$$Q_P(D_P) = \frac{3\varepsilon_P}{1+\varepsilon_P}\pi\varepsilon_0 D_P^2 E_{chg} \qquad (16)$$

Where E_{chg} is the mean electric field strength at the particle charging section.

f- Particle removal efficiency

The main objective of the present model is to determine the mass removal efficiency of particles. After finding the particle velocity and the concentration distribution one can derive the mass removal efficiency of particles by the following equation:

$$\eta = \frac{\left.\oint \int_{D_{P\,min}}^{D_{P\,max}} \rho_{Pa} \frac{\pi}{6} D_P^3 C_P(D_P) u_P \, dD_P \, dA \right|_{exit}}{\left.\oint \int_{D_{P\,min}}^{D_{P\,max}} \rho_{Pa} \frac{\pi}{6} D_P^3 C_{P0}(D_P) u_{P0} \, dD_P \, dA \right|_{entrance}}$$

(17)

2) Lagrangian model

The Lagrangian method is based on tracking individual particles from inlet to outlet of the ESP channel. In this study, the trajectories of 1500 particles, which were supposed to be located at starting points aligned at the inlet of the channel, were evaluated using equation 5. The particles, which hit the collecting wall, are assumed to be collected as a particle layer. The efficiency of ESP was evaluated by computing the number of collected particles. In order to calculate the particle concentration distribution the PSI-CELL model was modified to include the effect of particle size distribution. The conventional form of the PSI-CELL model is as follows {Crowe et al. (1977) [1]}:

$$C_p = \sum_{j=1}^{n_P} \frac{n_j \tau_j}{V_{C.V.}} \qquad (18)$$

Where n_j is number flow rate of particles at location j, τ_j is the residence time of particles in the control volume and $V_{C.V.}$ is the volume of control volume and n_P is the total number of trejectories passing this control volume. Since in the PSI-CELL model it is assumed that the gas velocity fluctuations do not influence the particle movement, the number flow rate of particles located at point j is constant along their trajectory. Thus the equation 17 can be written in the following form:

$$C_p = \sum_{j=1}^{n_P} \frac{u_{P0(j)} \Delta_{P(j)} C_{P0(j)} \tau_j}{V_{C.V.}} \qquad (19)$$

Where $u_{P0(j)}$ and $C_{P0(j)}$ are the initial velocity and concentration of particles located at point j and $\Delta_{P(j)}$ is the increment selected for location j. This equation was modified to include the effect of particle size distribution as follows:

$$C_P(D_P) = \sum_{j=1}^{n_P} \frac{u_{P0(j)} \Delta_{P(j)} C_{P0(j)}(D_P) \tau_j}{V_{C.V.}}$$

(20)

In this model the effect of gas turbulence on particle movement is ignored.

Method of solution

Figure 2 shows the algorithm used to solve the governing equations. Equation 1 (particle continuity) was solved by using power-law method of control volume. Equations 7 through 13 (Fluid flow) were solved by using the control volume method and SIMPLER algorithm. Equation 14 and 15 (electrical field) were solved by using the finite difference method. A grid with 160×60 cells was used to solve above equations. The staggered system was used to evaluate electrical field strength. The integrals appearing in equations 7, 8 and 14 were calculated by using fifth-order Gauss-Quadrature numerical integration method.

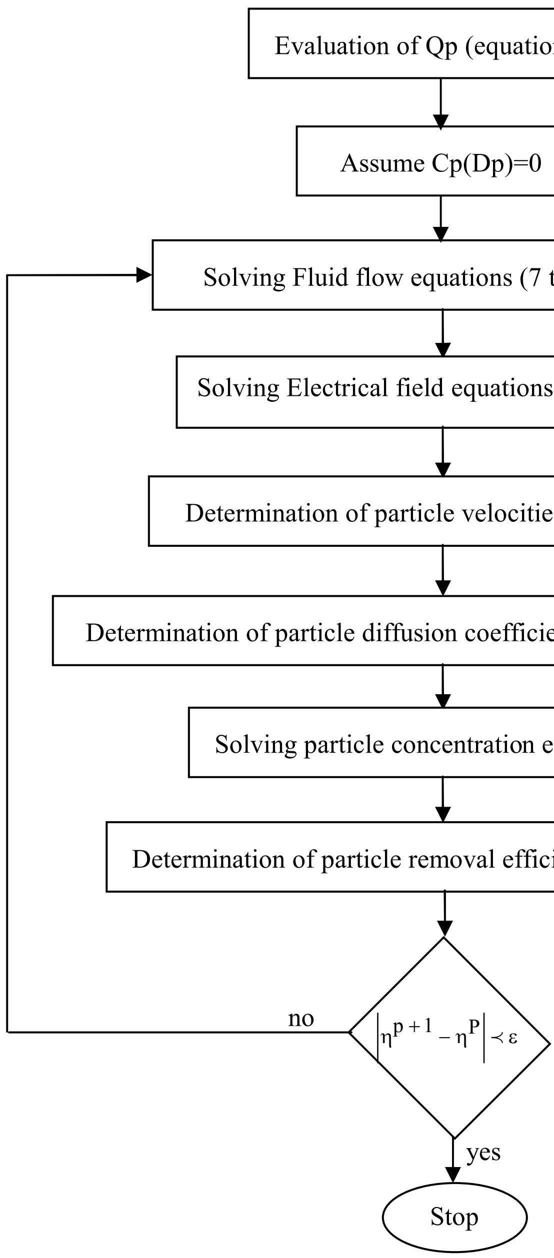

Figure 2. Algorithm used to solve the governing equations

Results

In order to verify the results of the mathematical model the experimental data of Leonard et al. (1980) [4] was used. In this experiment, oleic acid drops with a mean diameter of 3.5 μm and standard deviation (s) of 1.07 are removed from a gas stream by a double-stage ESP. Figure 3 shows the schematic configuration of the ESP used in this experiment. Figure 4 shows the results of the simulation of fluid flow for this experiment. Figure 5 shows the comparison between the results of the model and experimental data for particle dispersion. The results of the model based on the Eulerian approach are in good agreement with experimental data for C1=0.1. The parameter C1 in equation 3, has been determined in an experiment for heat transfer by Launder (1978) [3]. It can take values ranging from 0.2 to 0.4. This difference can be attributed to the weak prediction of turbulence intensity when using normal k-ε model. In the experiment of Leonard et al. (1980) [4], it was reported that, for the configuration of figure 3 at the distancce X=30 cm, the measured value of turbulence intensity was 12% while the value predicted using the normal k-ε model is 16%. According to equation 3, Ep is proportional to u'^4. If the measured value of turbulence intensity is used, the value of 0.33 is obtained for C1. This means that if a more accurate turbulence model were used, the value of 0.33, which is within an acceptable range, would be calculated for C1. As can be seen in figure 5, the model based on the simple Lagrangian approach, without considering the effect of gas turbulence, cannot predict particle movements in an ESP well. It can be attributed to the effect of gas turbulence on particle dispersion. Resulting from the use of baffles, the gas turbulence is high and particles are dispersed due to turbulent diffusion. Thus it is clear that the results reported by Suh and Kim (1996)[9] in which a simple Lagrangian approach has been used, may have some errors.

The strengtheners can be considered as several baffles in series along the collecting wall. In order to investigate the effect of wall strengtheners on the ESP's performance, the results of the model for a double-stage ESP with a ribbon as a baffle on the collecting wall were obtained. The following specifications were considered: applied voltage of 40 kV, inlet gas velocity of 2 m/s, particle density 2350 kg/m^3, inlet particle loading 5×10^{-7} kg/m^3, width of the ESP's channel 0.5 m and the baffle was set at 2.5 cm of the entrance. Figure 6 shows the contour plot of flow streamlines for a ribbon with 0.2 m height. Figures 7 through 10 show the cumulative variation of particle removal efficiency along the length of the ESP for different particle sizes. As can be seen, the effect of baffle depends on particle diameter. At low particle diameters the baffle increases particle removal efficiency (for D_P=2 and 5 μm). With increasing particle diameter, the negative effect of baffle is observed. In other words, the baffle decreases particle removal efficiency for large particle sizes (for D_P=10 and 20 μm). As is apparent in these figures, the sudden increase in the cumulative removal efficiency curve at a point 2.5 m from the entrance represents the impaction of particles on the front side of the ribbon. This effect can compensate the negative effect of the baffle on the particle removal efficiency to some extent. Figures 11 through 14 show the effect of baffle length on the particle removal efficiency for particle diameters of 2, 5, 10 and 20 μm. The specifications used to obtain these results are similar to the previous case. The lengths of baffle used are 1, 3, 5 and 7 m. As is apparent in these figures, increasing the length of the baffle increases particle removal efficiency. Figure 15 was created to explain this effect. This figure shows the variation of particle removal efficiency with the plate-plate distance or the spacing of ESP's channel at constant gas flow rate. This figure was obtained for an

ESP with the following specifications: length of ESP 5 m, particle diameter 10 μm, gas flow rate 1 m^3/s per m of ESP width, applied voltage 30 kV, particle density of 2350 kg/m^3 and inlet particle loading 5×10^{-7} kg/m^3.
Figure 15 shows that decreasing the plate-plate distance increases the particle removal efficiency. Decreasing the plate-plate distance has two effects. It increases the gas velocity which, in turn, has a decreasing effect on the removal efficiency. However, it increases the electric field strength and also reduces the total path for particles to be collected on collecting wall. These effects cause an increase in the removal efficiency. The net result of reducing spacing is to increase the particle removal efficiency.
One of the main effects of a baffle is to reduce the plate-plate distance along the length of the baffle, so it is clear that using longer baffle causes an increase in removal efficiency.
From result of the model represented in figure 15, the question can arise of how much the plate-plate distance can be reduced to augment the ESP performance. In order to answer this question, the third effect of decreasing plate-plate distance should be considered. For larger plate-plate distances, a lower pressure drop is obtained due to lower gas velocity. This, in turn, causes a lower operating cost. Therefore, a comprehensive economical optimization is required to obtain the optimum size of plate-plate distance.
The results shown in figure 15 can be also used to explain why baffles increase the collection efficiencies of small particles. As mentioned, the main effects of baffles is to increase the electrical force due to increase of electrical field strength and to change the inertia of particles due to distortion of fluid flow. The separation of particles from the gas stream depends mainly on the ratio of electric force to inertia. This ratio is proportional to the area to volume ratio of a particle (for spherical particles this ratio is equal to 6/Dp). Because this ratio is higher for small particles, the negative effect of baffles can be less than their positive effect on the separation of small particles. The net result can be to increase collection efficiency.

Conclusions

A mathematical model was developed to predict double-stage ESP performance. The effect of particle charge and movement on fluid flow and electrical field are considered in this model. Also, the influence of turbulence on particle movement was included by using a modified Eulerian approach.
The electrical field was determined by solving the Poisson equation including the effect of particle charge. The normal k-ε turbulent model with considering an electrical body force was used to predict the fluid flow field. Two methods (Eulerian and Lagrangian) were used to predict particle movement over the ESP. The model based on an Eulerian approach was used to investigate the effect of collecting wall strengtheners on ESP performance because the results showed that simple Lagrangian method could not represent the ESP performance well when a baffle was present. From the results of the model the following conclusions can be made:

1- Baffles introduce more turbulence and severe velocity distribution to the fluid. Turbulence dispersion of particles decreases removal efficiency. Also the effect of gas turbulence on particle dispersion cannot be ignored.
2- Baffles can have a positive effect on particle removal efficiency depending on particle diameter. For low particle diameters the presence of baffles increases the removal efficiency. However, for large particle size baffles cause a decrease collection efficiency.
3- Increasing the length of a baffle increases removal efficiency.

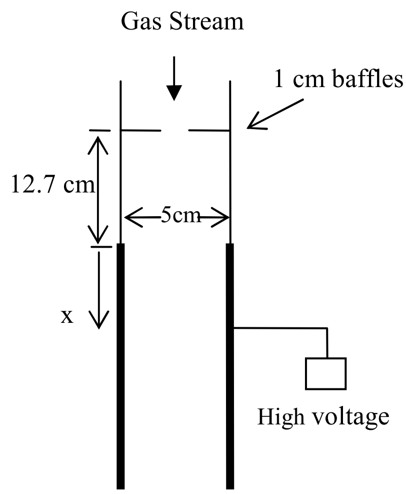

Figure 3. Schematic configuration of the ESP used in the Leonard experiment.(1982)

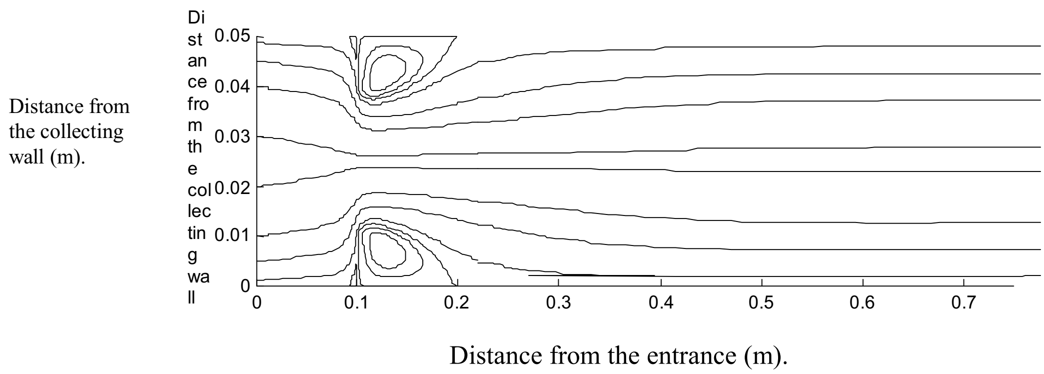

Figure 4. The result of simulation of fluid flow for Leonard (1982) experiment

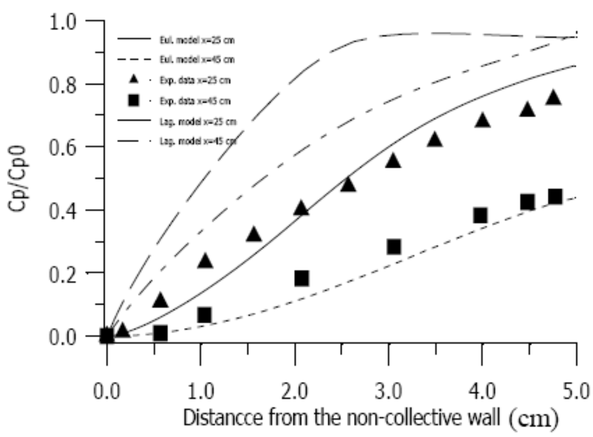

Figure 5. Comparison between the results of the model and experimental data of Leonard (1982).

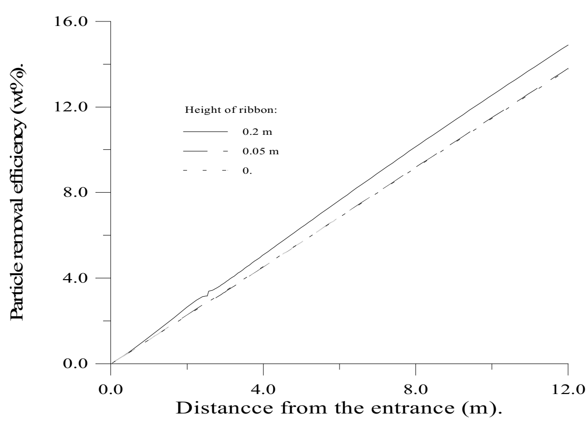

Figure 6. Contour plot of gas streamline for a double-stage ESP with a ribbon of 0.2 m height at 2.5 m from the entrance.

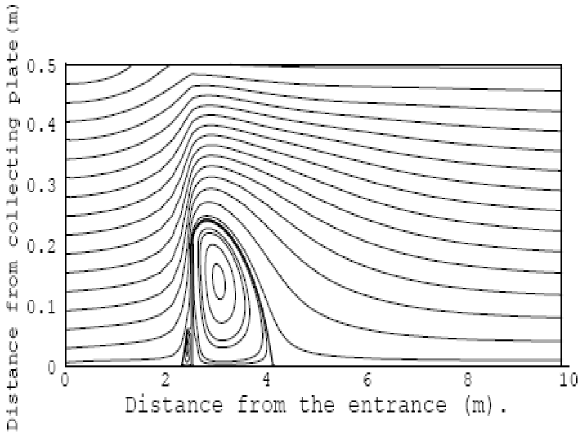

Figure 7. The cumulative variation of particle removal efficiency with length of the ESP's channel for D_P= 2 μm.

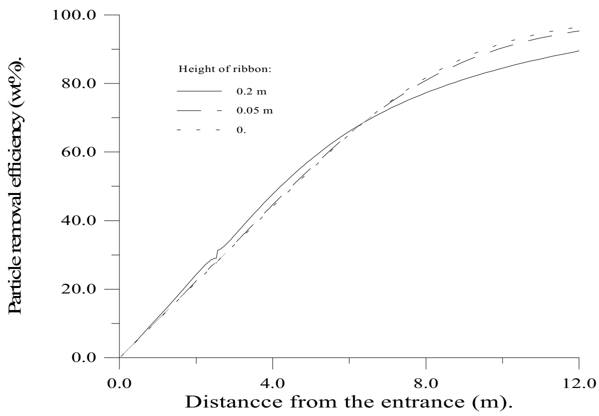

Figure 10. The cumulative variation of particle removal efficiency with length of the ESP's channel for D_P= 20 μm.

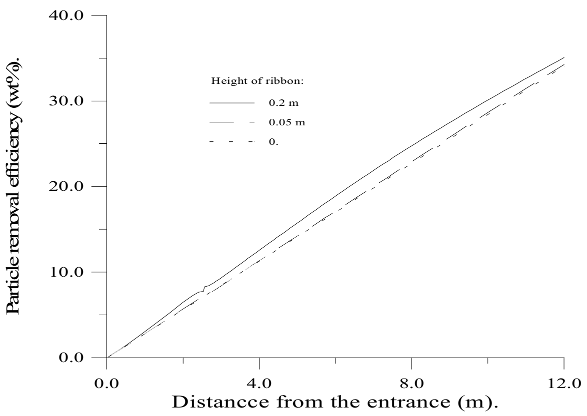

Figure 8. The cumulative variation of particle removal efficiency with length of the ESP's channel for D_P= 5 μm.

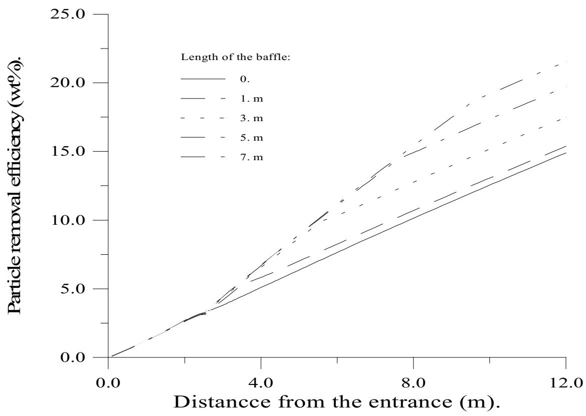

Figure 11. The cumulative variation of particle removal efficiency with length of the ESP's channel for D_P= 2 μm.

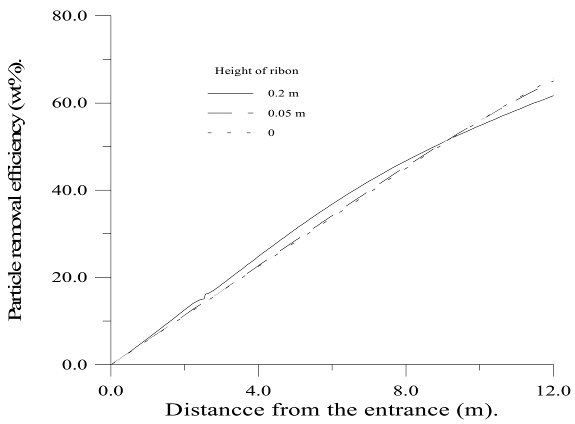

Figure 9. The cumulative variation of particle removal efficiency with length of the ESP's channel for D_P= 10 μm.

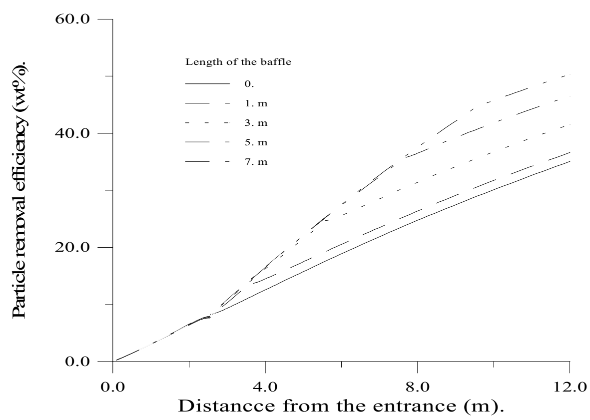

Figure 12. The cumulative variation of particle removal efficiency with length of the ESP's channel for D_P= 5 μm.

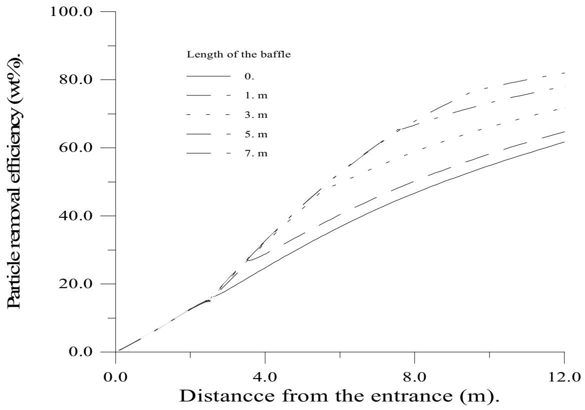

Figure 13. The cumulative variation of particle removal efficiency with length of the ESP's channel for D_P= 10 μm.

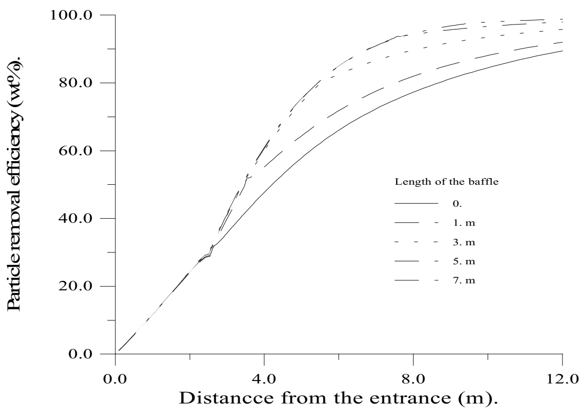

Figure 14. The cumulative variation of particle removal efficiency with length of the ESP's channel for D_P= 20 μm.

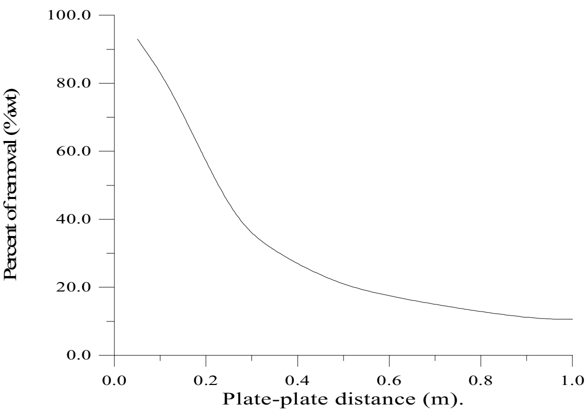

Figure 15. The variation of particle removal efficiency with plate-plate distance for D_P= 10 μm.

Nomenclature

C_P	Number concentration of particles with diameter D_P	(No./m^3)
$C_P(D_P)$	Number frequency distribution of particle size	(No./m^4)
C_{P0}	Number concentration of particles with diameter D_P at entrance	(No./m^3)
C_{P0t}	Total number concentration of particles at entrance	(No./m^4)
$C_{P0}(D_P)$	Number frequency distribution of particle size at entrance	(No./m^4)
$C_{Pn}(D_P)$	Number frequency distribution of particle size at collecting wall	(No./m^4)
D_P	Particle diameter	(m)
E	Electric field strength	(V/m)
E_{chg}	Electric field strength at particle charging section	(V/m)
E_p	Particle diffusivity coefficient	(m^2/s)
k	Turbulence kinetic energy	(J/s/kg)
$Qp(D_P)$	Electric charge of particles having diameter between D_P and D_P+dD_P	(C)
u	x-component fluid velocity	(m/s)
U	Fluid velocity vector	(m/s)
u_p	x-component particle velocity	(m/s)
U_p	Particle velocity vector	(m/s)
v	y-component fluid velocity	(m/s)
v_p	y-component particle velocity	(m/s)
x	x direction	(m)
y	y direction	(m)

Greek letters

ρ_f	Fluid density	(kg/m^3)
ρ_{Pa}	Particle density	(kg/m^3)
ε	Turbulence dissipation rate	(J/s/kg)
ε_0	Permittivity of free air	(8.854×10^{-6} F/m)
ε_p	Relative permittivity	(Dimensionless)
ϕ	Electric potential	(V)
ϕ_w	Applied voltage	(V)
μ	Laminar viscosity	(kg/ms)
μ_t	Turbulent viscosity	(kg/ms)
η	Mass removal efficiency of particles	(Dimensionless)

References

1- Crowe, C. T., M. P. Sharma and D. E. Stock, (1977), "The particle-source-in-cell (PSI-CELL) model for gas-droplet flows," Trans. ASME, J. Fluids Eng., pp. 235.

2- Goo, JH. and JW. Lee, (1997), "Stochastic simulation of particle charging and collection Characteristic for a wire-plate electrostatic precipitator of short length," Journal of Aerosol Science, 28(5), pp. 875-893.

3- Launder, B. E., *Topics in Applied Physics: Turbulence*, Ch. 6, pp 231-287, Springer, (1978).

4- Leonard, G. L., M. Mitchner and S. A. Self, (1983), "An experimental study of electrohydrodynamic flow in electrostatic precipitators," Journal of Fluid Mechanics, 127, pp. 123-140.

5- Lowe, H. J., (1969), "Reduction of emissions of pollutants," Phil. Trans. R. Soc. Lond., A 265, 301.

6- Sartor, J. D. and Abbott, C. E., (1975), "Prediction and measurement of the accelerated motion of water drops in air," Journal of Applied Meteorology, 14, pp. 232-239.

7- Stenhouse, J. I. T. and K. Barnes, (1990), "Aerosol deposition in electrostatic precipitators," J. Aerosol Science, 25, S329.

8- Suh, Y. J. and S. S. Kim, (1995), "The effect of baffles on the particle collection efficiency in a two-stage electrostatic precipitator," Proc. KSME Thermal & Fluid Engineering Division, p. 124.

9- Suh, Y. J. and S. S. Kim, (1996), "Effect of obstructions on the particle collection efficiency in a two-stage electrostatic precipitator," J. Aerosol Science 25(1), pp 61-74.

10- Talaie, M. R., J. Fathikalajahi and M. Taheri, (2001), "Mathematical modeling of doublestage electrostatic precipitators based on a new Eulerian approach," Journal of Aerosol Science & Technology, 34, pp. 512-519.

11- Tennekes, H. and J. L. Lumby, (1972), *A first course in turbulence,* MIT Press, Cambridge, Massachusetts.

12- Vincent. J. H. and A. S. M. McLennan, (1980), "Aerodynamic considerations in electrostatic precipitation," J. of Electrostatics, 8, 325.

13- White, H. J., (1963), *Industrial electrostatic precipitation*, Addison-Wesley, Reading, MA, Ch.6.